Work extraction from single-mode thermal noise by measurements: How important is information?

Avijit Misra [*]
AMOS and Department of Chemical and Biological Physics, Weizmann Institute of Science, Rehovot 7610001, Israel
and International Center of Quantum Artificial Intelligence for Science and Technology (QuArtist) and Department of Physics, Shanghai University, 200444 Shanghai, China

Tomáš Opatrný [†]
Department of Optics, Faculty of Science, Palacký University, 17. listopadu 50, 77146 Olomouc, Czech Republic

Gershon Kurizki [‡]
AMOS and Department of Chemical and Biological Physics, Weizmann Institute of Science, Rehovot 7610001, Israel

(Received 8 September 2022; accepted 18 October 2022; published 14 November 2022)

Our goal in this article is to elucidate the rapport of work and information in the context of a minimal quantum-mechanical setup: a converter of heat input to work output, the input consisting of a single oscillator mode prepared in a hot thermal state along with a few much colder oscillator modes. The core issues we consider, taking account of the quantum nature of the setup, are as follows: (i) How and to what extent can information act as a work resource or, conversely, be redundant for work extraction? (ii) What is the optimal way of extracting work via information acquired by measurements? (iii) What is the bearing of information on the efficiency-power tradeoff achievable in such setups? We compare the efficiency of work extraction and the limitations of power in our minimal setup by different, generic, measurement strategies of the hot and cold modes. For each strategy, the rapport of work and information extraction is found and the cost of information erasure is allowed for. The possibilities of work extraction without information acquisition, via nonselective measurements, are also analyzed. Overall, we present, by generalizing a method based on optimized homodyning that we have recently proposed, the following insight: extraction of work by observation and feedforward that only measures a *small fraction* of the input is clearly advantageous to the conceivable alternatives. Our results may become the basis of a practical strategy of converting thermal noise to useful work in optical setups, such as coherent amplifiers of thermal light, as well as in their optomechanical and photovoltaic counterparts.

DOI: 10.1103/PhysRevE.106.054131

I. INTRODUCTION

Thermal noise, i.e., maximal-entropy fluctuation at a given temperature, is a ubiquitous source of propagating energy, ranging from sunlight and cosmic rays to acoustic (e.g., seismic) energy. Since the invention of the steam engine, technology has aimed at harnessing thermal noise (heat) for the performance of useful work. The definition of work in the literature is elusive, but it may be loosely phrased as the most ordered energy, or, more formally, as energy exchange with the least (ideally zero) entropy exchange. The question to be posed is, what is the *most efficient way* of accomplishing such heat-to-work conversion? Not less importantly, what is the *fastest way* of converting heat to work, thereby attaining the maximal rate of work production, also known as *maximal power*?

The conversion of heat to work consists in lowering the entropy from its highest to its lowest value at a given energy within the constraints of the first and second laws of thermodynamics [1]. Such conversion is a central theme that quantum thermodynamics (QTD) has inherited from its classical predecessor [2–9], the difference being that QTD accounts for possible effects of coherence and entanglement in heat engine (HE) designs [10–39]. A conceptual alternative to an HE has been provided by information engines (IEs) originating from Maxwell-demon [40] and Szilard engines [41–44], which exploit information acquired by measurements as a resource complementary to heat. Both HEs and IEs have merits but also basic limitations, the central one being power-efficiency tradeoff: In an HE it is inevitable for power to diminish near the point of maximum efficiency, which is always bounded by the Carnot limit in accordance with the second law [1–8,35–39]. Commonly, IEs have been based on binary measurements of discrete variables, whose energetic price yields efficiency bounds well below unity [45–48]. On the other hand, the duration of work extraction from IEs is not intrinsically related to the efficiency, so that their power-efficiency tradeoff may be in principle more favorable than in HEs, as indeed is shown here.

Our goal is to elucidate the rapport of work and information in the context of a minimal quantum-mechanical setup: a

[*]avijit.misra@weizmann.ac.il
[†]tomas.opatrny@upol.cz
[‡]gershon.kurizki@weizmann.ac.il

converter of heat input to work output, the input consisting of a single oscillator mode prepared in a hot thermal state. In particular, we measure the input, and we exploit the measured results as feedforward for work extraction. Taking account of the quantum nature of the setup, the acquisition of information by *measurements*, its cost and utilization for our purpose raise the following core issues: (i) How and to what extent can information act as a work resource, or, conversely, be redundant for work extraction? (ii) What is the optimal way of extracting work via information acquired by measurements? (iii) What is the bearing of information on the efficiency-power tradeoff achievable in such setups?

To address these questions, we resort to nonequilibrium heat-to-work conversion in terms of ergotropy (nonpassivity, Appendix A) [2,7,8,25,28,49–56]. We then compare the efficiency of work extraction and the limitations of power in our minimal setup by different, generic, measurement strategies of the hot and cold modes (Secs. II–IV), finding for each strategy the rapport of work and information extraction and allowing for the cost of information erasure. The possibilities of work extraction without information acquisition, via nonselective measurements, are analyzed (Sec. V). The findings are summarized in the Conclusion (Sec. VI).

Overall, we present, by generalization of a method based on optimized homodyning we have recently proposed [57], the following insight: extraction of work by observation and feedforward (WOF) that only measures a *small fraction* of the input is clearly advantageous compared with the conceivable alternatives. As discussed in the Conclusion, our results may become the basis of a practical strategy of converting thermal noise to useful work in optical setups, such as coherent amplifiers of thermal light, as well as in their optomechanical [54] and photovoltaic [58] counterparts.

II. WORK EXTRACTION BY OBSERVATION AND FEEDFORWARD FROM A THERMAL MODE

To circumvent the tradeoff between efficiency and power that is inherent in heat engines, one may consider information engines (IEs) whose power is determined by the measurement duration and the detector resetting time.

For the minimal scheme of a single hot mode considered here, the need for an IE arises since its passive (particularly thermal) state cannot be used for extracting work by unitary transformations (Appendix A). Namely, we need to measure the state and apply feedforward to extract work from the information. We shall present our idea concerning work extraction from a thermal state via quantum measurements that probe only a *small fraction* of the input so as to minimize the measurement cost and feedforward of the acquired information in order to steer the unmeasured (dominant) fraction at low cost.

Several methods based on what we have dubbed [57] "work by observation and feedforward (WOF)" will be compared in the following subsections.

A. WOF by energy measurement of the entire thermal field

If one performs sufficiently many energy measurements of the thermal oscillator mode and transforms each time the postmeasured state to the ground state, the work extracted from the ensemble is the average energy of the oscillator,

$$\langle E\rangle = \hbar\omega\bar{n}. \tag{1}$$

The ideal extraction method consists of many quantum nondemolition (QND) Fock-state measurements, i.e., $|n\rangle\langle n|$ projectors, each projection followed by displacement (downshift) to the ground (vacuum) state $|0\rangle$ via the unitary operation $|0\rangle\langle n| + |n\rangle\langle 0|$. Such operations are hard to implement, even conceptually. In what follows, we do not discuss such QND operations, but rather realistic, finite accuracy measurements that result in dispersion (spread) in the number-state basis.

We are only concerned here with the fundamental cost of detector resetting as opposed to the cost of idealized projective measurement [59] that bears infinite cost and time. According to Landauer's erasure principle [42], the energetic cost of resetting a detector that is kept in an environment at temperature T_D is given by the amount

$$Q_D = k_B T_D I_D \tag{2}$$

that is proportional to its entropy increase I_D.

We find (Appendix E) that the detector entropy increase is the same as the entropy of the input thermal distribution,

$$\begin{aligned} S(\bar{n}) &= k_B[(\bar{n}+1)\ln(\bar{n}+1) - \bar{n}\ln\bar{n}],\\ I_D &= S(\bar{n})/k_B = 1 + \ln\bar{n} \text{ for } \bar{n} \gg 1. \end{aligned} \tag{3}$$

The net work gained is therefore bounded by

$$W = \langle E\rangle - Q_D. \tag{4}$$

Thus, for $T_D \simeq T_h$, WOF by *energy measurement of the entire input is an inefficient method* that wastes most of the gained work on the detector heat up. The only way to gain work by this method is to lower the temperature T_D compared to the input (hot-mode) temperature T_h in order to achieve $W \gg Q_D$. Furthermore, as discussed in this section, the cost of feedforward that is required to extract work from the postmeasured state increases with the information gain. To remedy these drawbacks, we proposed [57] to lower the entropy increase of the detector (and not only to reduce the environmental temperature T_D to minimize the resetting cost) by measuring only a small fraction of the input, as shown in Secs. II B, II C, and IV B.

B. WOF by small-fraction photocount

Here, we study work extraction from a thermal field mode by detecting a small fraction of the input in the Fock basis and extracting work from the postmeasured state. For an electromagnetic (EM) field mode, this corresponds to photocounts performed on the sampled (reflected) fraction (Fig. 1) of a thermal input incident on a beam splitter (BS) with high transmissivity κ^2.

A thermal state at the input temperature T_h (with mean quanta number $\bar{n}$) in the Fock basis is represented as

$$\rho(T_h) = \sum_n p_n|n\rangle\langle n|, \tag{5}$$

where $p_n = e^{-\frac{\hbar\omega n}{k_B T}}(1 - e^{-\frac{\hbar\omega}{k_B T}})$ is the occupancy of the nth Fock state. Detection of m-quanta of the reflected beam occurs

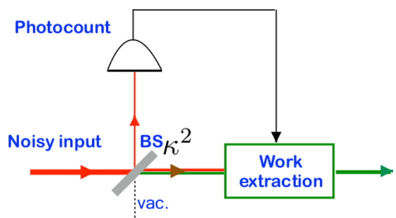

FIG. 1. Scheme of work extraction by quanta number detection (photocount) from a small fraction of a noisy input signal. The input is incident on a BS with high transmissivity κ^2, and the photocount is done on the reflected part. Work is extracted by unitary manipulation from the postmeasured transmitted part.

with a probability (Appendix C)

$$p_m = \left(1 - e^{-\frac{\hbar\omega}{k_B T'}}\right) e^{-\frac{\hbar\omega}{k_B T'} m}, \tag{6}$$

where we have introduced the effective temperature of the reflected beam

$$\exp\left(\frac{\hbar\omega}{k_B T'}\right) = \frac{\exp\left(\frac{\hbar\omega}{k_B T}\right) - \kappa^2}{1 - \kappa^2}. \tag{7}$$

This m-quanta detection yields the postmeasured (conditional) state that has transmitted through the high transmissivity BS

$$\begin{aligned} \rho_m &= \frac{1}{m!}\left(1 - e^{-\frac{\hbar\omega}{k_B T}}\kappa^2\right)^{m+1} \\ &\quad \times \left[\sum_{n=0}^{\infty} e^{-\frac{\hbar\omega}{k_B T} n} (\kappa^2)^n \frac{(n+m)!}{n!} |n\rangle\langle n|\right] \\ &= \sum_{n=0}^{\infty} p(n|m) |n\rangle\langle n|. \end{aligned} \tag{8}$$

The thermal distribution is modified in the postmeasured state depending on $\bar{n}$, κ^2, and the measurement outcome m (Appendix C, Fig. 2). The projection on the m-quanta state of the reflected beam can be geometrically represented by a ring in the phase plane that cuts out a hollow crater from the input thermal (Gaussian) distribution (Fig. 3). We observe the *nonmonotonicity of the postmeasured state distribution, which attests to nonpassivity* in Figs. 2 and 3, as the state, diagonal in Fock basis, in Eq. (8) is passive iff the probabilities satisfy [49]

$$p(n|m) \geqslant p(n'|m), \quad \forall n, n' \quad \text{when } E_n > E_{n'}. \tag{9}$$

The departure from the thermal character of the input is also manifested by the second-order coherence function [60] for the postmeasured state in Eq. (8), which can be evaluated to be

$$\begin{aligned} g^{(2)}(0) &= \frac{\langle a^{\dagger 2} a^2 \rangle}{\langle a^\dagger a \rangle^2} \\ &= \frac{\sum_{n=0}^{\infty} p(n|m)\, n(n-1)}{\bar{n}_m^2} \\ &= 1 + \frac{1}{1+m}. \end{aligned} \tag{10}$$

Thus, the second-order coherence function is *independent of the input beam temperature* and the splitting ratio of the BS. When no photon is detected, i.e., the entire beam passes through the BS, the transmitted beam is thermal as expected, with $g^{(2)}(0) = 2$. In the limit of a large number of detected quanta $m \gg 1$, $g^{(2)}(0)$ of the transmitted beam converges to $g^{(2)}(0) = 1$, indicating Poissonian statistics.

Work cannot be extracted by displacing the postmeasured state in Eq. (8), as its mean quadratures are zero (Appendix A). Instead, one can perform a (unitary) permutation in the Fock-basis such that the modified probabilities satisfy the passive-state condition Eq. (9). The average energy of the postmeasured state,

$$E_m = \hbar\omega \frac{(1+m)\kappa^2}{e^{\frac{\hbar\omega}{k_B T}} - \kappa^2}, \tag{11}$$

can always be lowered to E'_m by the permutation that renders the state passive, thereby extracting the amount of work

$$W_m = E_m - E'_m. \tag{12}$$

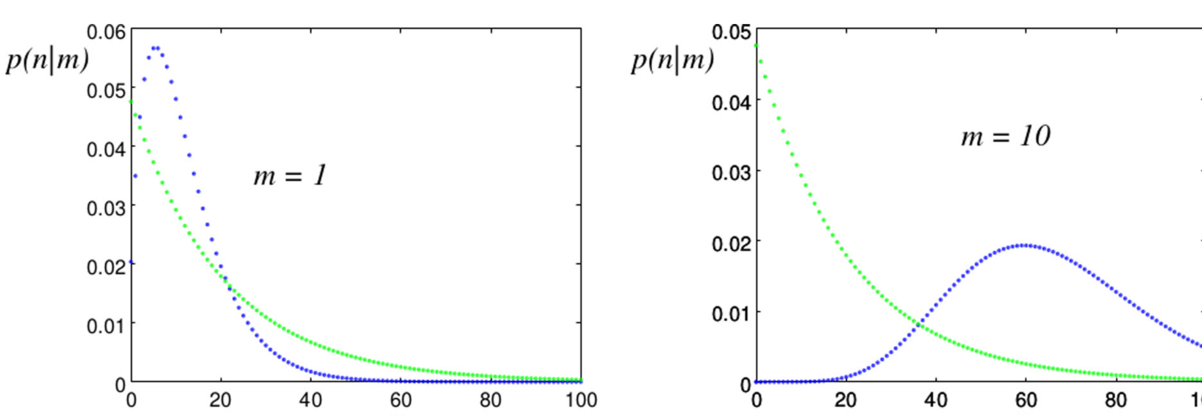

FIG. 2. The probabilities $p(n|m)$ (blue dots) of occupying the nth Fock state in the postmeasured [Eq. (8)] state when the measurement outcome is m quanta for a thermal input with a mean number of quanta $\bar{n} = 20$, and a BS with transmissivity $\kappa^2 = 0.9$. The plots clearly show that the occupation probabilities are nonmonotonic and therefore the postmeasured state is nonpassive. The green dots represent the quanta number distribution of the thermal input with a mean number of quanta $\bar{n} = 20$.

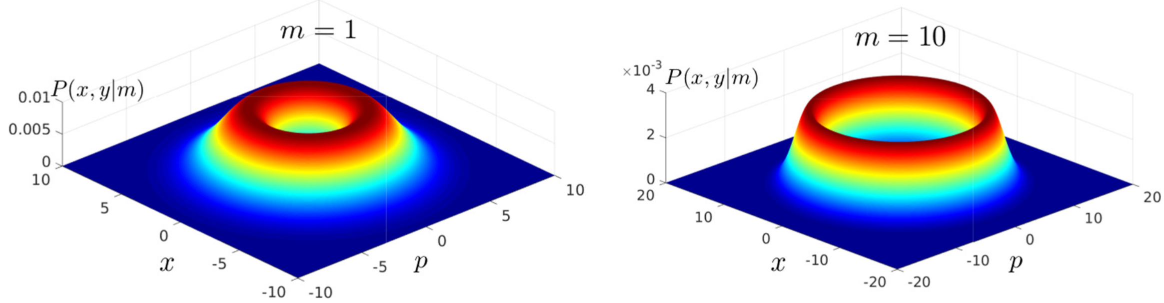

FIG. 3. The P-distribution of the postmeasured state for a thermal input with $\bar{n} = 20$ when the measurement outcome is m quanta (Appendix C): $m = 1$ (left) and $m = 10$ (right). The BS transmissivity $\kappa^2 = 0.9$. The plots clearly show the nonmonotonicity of the energy distribution, which implies nonpassivity.

Upon averaging over all outcomes m, the net work gain can be obtained as

$$W = \sum_m p_m W_m. \tag{13}$$

The efficiency of this photocount WOF and other WOF considered in this article is given by

$$\eta = \frac{W}{\hbar\omega\bar{n}}, \tag{14}$$

which is the ratio of work extracted to the hot mode energy. However, the efficiency must account for the resetting cost [Eqs. (2)–(4)].

We show in Sec. III C that the detector heat-up cost $Q_D = k_B T_D I_D$ [Eq. (18)] for small-fraction WOF can be made lower than its counterpart for entire energy measurement in Sec. II A. This cost can further be suppressed by choosing a much lower environmental temperature T_D for the detector than that of the hot mode. The practical merit of small-fraction photocount is that it is much easier to implement than the perfect QND measurement required in Sec. II A.

Our numerical results confirm that WOF by photocount of a small fraction can have higher efficiency than the entire energy measurement for a suitable BS transmissivity κ^2 and a given T_D. However, the inability to fully sample the phase-space distribution of the input in the Fock basis limits the efficiency. Practically, simple operations such as displacement cannot extract work in this scheme, as noted above. We therefore resort to WOF homodyning in Sec. III C.

C. WOF via phase-sensitive (homodyne) measurement of a small fraction

In the quantum domain, joint position and momentum measurements cannot be done perfectly and are limited by the quantum uncertainty. Nevertheless, we have shown that [57] a passive (thermal) signal can be used to efficiently extract work via homodyne measurements of its noncommuting orthogonal quadratures performed on a small fraction of the input and followed by information feedforward of the unmeasured dominant fraction. The open issue we address is, what is the rapport between work output and information gain in this scheme?

We first briefly present this scheme where the hot field mode is incident on a BS with high transmissivity κ, and a vacuum mode is incident on the other port of the BS (with low reflectivity $\sqrt{1-\kappa^2}$). Finite-temperature input instead of vacuum has been fully analyzed in the supplementary information of Ref. [57], the result being weak modification of the vacuum input case for low-temperature input.

A homodyne measurement is performed on the orthogonal quadratures of a small split fraction of the incoming field by mixing it with an equally small fraction of a local oscillator. The remaining (unmeasured) part of the hot-mode field is projected onto a state from which work can be extracted by a unitary transformation (displacement). We stress that the goal is not to remove as much heat as possible but to extract maximal work by maximizing ergotropy. This process is not equilibration with a zero-temperature bath but a maximal change in the state passivity by information acquisition, as detailed below.

A thermal state of a harmonic oscillator can be represented as a random mixture of coherent states $|\alpha\rangle$. Assume first that a coherent state $|\alpha\rangle$ with complex coherent amplitude $\alpha = \frac{1}{\sqrt{2}}(x + ip)$ enters the setup in Fig. 4. After the first BS with splitting ratio $\kappa^2/(1-\kappa^2)$, the state $|\kappa\alpha\rangle$ is transmitted and the state $|\sqrt{1-\kappa^2}\alpha\rangle$ is reflected towards the homodyne detectors for estimating the quadratures $\hat{x}$ and $\hat{p}$ of the input state. We resort to a local oscillator in a coherent state with

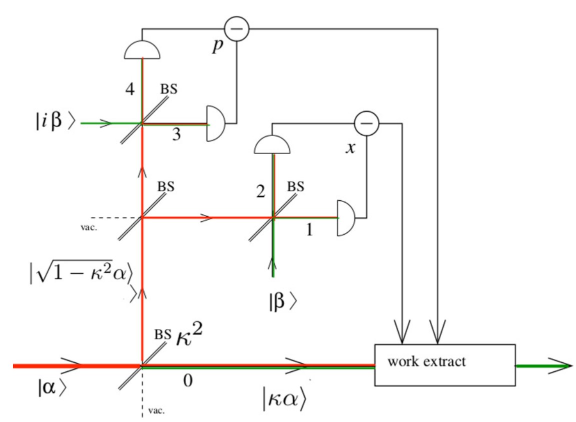

FIG. 4. Scheme of the setup for WOF by small-fraction homodyning: an unknown state (here labeled as coherent state $|\alpha\rangle$) enters a beam splitter, which transmits a fraction κ^2 of the input energy and reflects $\sqrt{1-\kappa^2}$. On the reflected part, a homodyne measurement is performed to estimate the quadratures x and p.

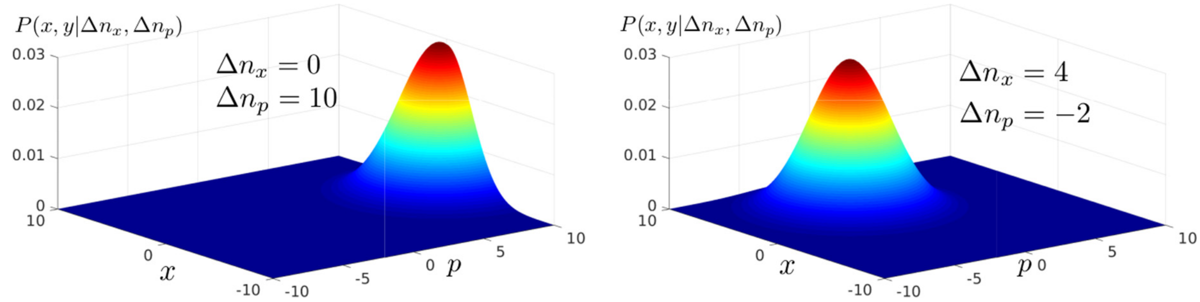

FIG. 5. The P-distribution of the postmeasured state for a thermal input with $\bar{n} = 16$ when the measurement outcomes are Δn_x and Δn_p. The BS transmissivity $\kappa^2 = 0.75$ and $\beta = 1.4$.

real quadrature-amplitude β and to its imaginary quadrature counterpart with amplitude $i\beta$. The modes 0,1,2,3,4 behind the BS are in a multimode (product) coherent state. The photocount differences $\Delta n_x \equiv n_1 - n_2$ and $\Delta n_p \equiv n_3 - n_4$ in Fig. 4 carry information on the input-field quadratures x and p [57].

Let us now take the input state to be a mixture of coherent states,

$$\hat{\varrho} = \int\int P(\alpha)|\alpha\rangle\langle\alpha|d^2\alpha. \tag{15}$$

For a thermal input state with a mean number of quanta $\bar{n}$, the Glauber-Sudarshan phase-space distribution is Gaussian in the quadratures,

$$\begin{aligned} P(\alpha) &= \frac{1}{\pi\bar{n}}\exp\left(-\frac{|\alpha|^2}{\bar{n}}\right) \\ &\equiv P(x,p) = \frac{1}{2\pi\bar{n}}\exp\left(-\frac{x^2+p^2}{2\bar{n}}\right). \end{aligned} \tag{16}$$

The distribution of α (see Fig. 5), conditioned on the detection of quanta number differences Δn_x and Δn_p, is [57]

$$P(\alpha|\Delta n_x,\Delta n_p) = \frac{p(\Delta n_x,\Delta n_p|\alpha)P(\alpha)}{p(\Delta n_x,\Delta n_p)}. \tag{17}$$

The unmeasured (transmitted) field mode has the state (conditional on the detection of Δn_x and Δn_p)

$$\hat{\varrho}(\Delta n_x,\Delta n_p) = \frac{1}{\kappa^2}\int\int P\left(\frac{\alpha}{\kappa}|\Delta n_x,\Delta n_p\right)|\alpha\rangle\langle\alpha|d^2\alpha. \tag{18}$$

This state has in general *nonvanishing mean values* of quadratures $\hat{x}$ and $\hat{p}$,

$$\begin{aligned} \langle\hat{x}\rangle &= \kappa\int\int xP(\alpha|\Delta n_x,\Delta n_p)d^2\alpha, \\ \langle\hat{p}\rangle &= \kappa\int\int pP(\alpha|\Delta n_x,\Delta n_p)d^2\alpha. \end{aligned} \tag{19}$$

A great merit of this scheme is that one can extract most of the stored work (albeit not fully [57]) by simply downshifting (displacing to the origin) the state [Eq. (18)] such that the mean quadratures of the final state are zero. The mean work obtained in this process can be found by averaging $\frac{\hbar\omega}{2}(\langle\hat{x}\rangle^2 + \langle\hat{p}\rangle^2)$ over all values of Δn_x, Δn_p, and *subtracting the invested energy of the two local oscillators* $2\hbar\omega\beta^2$. The extractable work is then found to be

$$\begin{aligned} W &\approx \frac{\hbar\omega}{2}\int\int(\langle\hat{x}\rangle^2 + \langle\hat{p}\rangle^2)p(\Delta n_x,\Delta n_p)d\Delta n_x d\Delta n_p - 2\hbar\omega\beta^2 \\ &\approx 2\hbar\omega\beta^2\left[\frac{\kappa^2(1-\kappa^2)\bar{n}^2}{2\beta^2 + (1-\kappa^2)(1+2\beta^2)\bar{n}} - 1\right]. \end{aligned} \tag{20}$$

The expression can be optimized with respect to β and κ (Appendix E). The resulting maximal work gained by using the information as feedforward to downshift the unmeasured part is

$$W_{\max} \approx \hbar\omega\left(\sqrt{\bar{n} - \sqrt{\bar{n}} + 1} - 1\right)^2\left(1 - \frac{1}{\sqrt{\bar{n}}}\right). \tag{21}$$

For large $\bar{n}$, the optimized values of the BS transmissivity and local oscillator energy read as $1 - \kappa^2 = \frac{1}{\sqrt{\bar{n}}}$ and $2\beta^2 = \sqrt{\bar{n}}$, respectively, and the maximal extractable work is given by

$$W_{\max} \approx \hbar\omega\left[\bar{n} - 4\sqrt{\bar{n}} + 6 + O\left(\frac{1}{\sqrt{\bar{n}}},\frac{1}{\bar{n}}\right)\right]. \tag{22}$$

In Fig. 6 we compare the efficiency in the small-fraction WOF homodyning scheme with that of small-fraction photocount in Sec. II B. In photocount we do not obtain phase

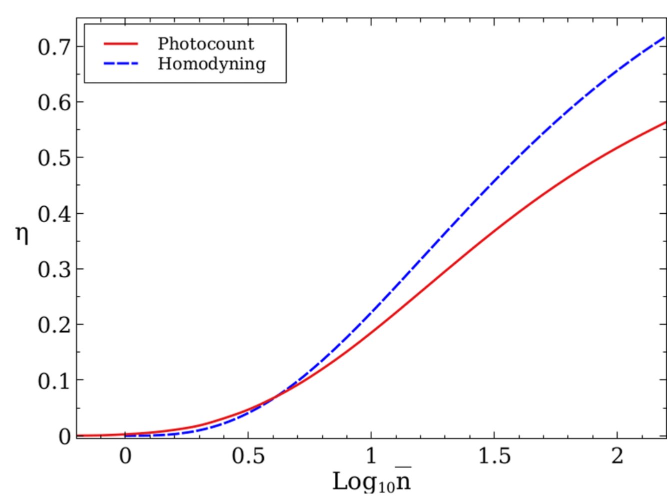

FIG. 6. Efficiency $\eta = W/\hbar\omega\bar{n}$ of extractable work by small-fraction photocount WOF compared to small-fraction homodyne WOF as a function of the mean input quanta number $\bar{n}$. The BS transmissivity for the photocount scheme is $\kappa^2 = 0.75$.

information, only number-state probabilities, hence the work extraction and its efficiency are expected to be lower than by homodyning. However, this turns out to be true only for large $\bar{n}$. This is due to *the local oscillator energy* invested in homodyning WOF, whereby *much of the work is wasted for small $\bar{n}$,* in contrast to photocount.

III. WOF INFORMATION ERASURE AND FEEDFORWARD CONSIDERATIONS

The work information tradeoff in any realistic IE [45,46] is dependent on the cost of information erasure (resetting) discussed in Secs. IV C–IV E and feedforward cost in Secs. IV A and IV B. The latter, however, is specific to the concrete implementation and cannot be generally quantified. Yet, the lower bound on the feedforward cost is determined by the information gained by the measurement, also known as mutual information.

A. Mutual information and feedforward cost bound

Let us calculate the information gain, characterized by the mutual information [45,46], that needs to be processed for feedforward in this WOF. If the input is in a state n and we get a measurement outcome m with probability $p(m)$, then the pointwise mutual information

$$\mathcal{I}_{\rm mn} = \ln p(m|n) - \ln p(m) \tag{23}$$

quantifies the uncertainty reduction or equivalently information gain by the measurement outcome m [61]. Here $p(m|n)$ is the conditional probability, and $-\ln p(m)$ quantifies the uncertainty in the measurement outcome m. If we average this pointwise mutual information over the joint probability distribution $p(m,n)$, we get the total mutual information which quantifies the correlation between the input statistics of the measured system and the outcomes [61], i.e.,

$$\mathcal{I} = \sum_{m,n} p(m,n)\mathcal{I}_{\rm mn}. \tag{24}$$

Equivalently, the mutual information can be expressed in terms of the corresponding entropies as (Appendix F)

$$\mathcal{I} = -\sum_{n} p(n)S(p(m|n)) + S(p(m)). \tag{25}$$

This information gain needs to be processed for work extraction via feedforward. The feedforward cost associated with the information gain has the lower bound [62]

$$E_F \geqslant k_B T_D \mathcal{I} \tag{26}$$

when the information is processed at an environmental temperature T_D.

B. Mutual information and feedforward cost bound for small-fraction homodyne WOF

Let us calculate the information gain, characterized by the mutual information [45,46], that needs to be processed for feedforward in this small-fraction homodyne WOF. The average mutual information can be expressed as (Appendix F)

$$\begin{aligned}\mathcal{I} &= \iiint \int \ln \frac{P(x,p|\Delta n_x,\Delta n_p)}{P(x,p)} P(x,p|\Delta n_x,\Delta n_p) \\ &\quad \times p(\Delta n_x,\Delta n_p) d\Delta n_x d\Delta n_p dx dp \\ &= \langle I_x\rangle + \langle I_p\rangle, \end{aligned}\tag{27}$$

as the joint probabilities factorize in x and p, where

$$\langle \mathcal{I}_x\rangle = \iint \ln \frac{P(x|\Delta n_x)}{P(x)} P(x,|\Delta n_x) p(\Delta n_x) d\Delta n_x dx = \langle \mathcal{I}_p\rangle. \tag{28}$$

Using the optimized values of β and κ for maximum work extraction (Appendix E), we obtain for $\bar{n} \gg 1$

$$\langle \mathcal{I}_x\rangle \approx -\frac{1}{2}\ln\left(1 - \frac{\bar{n}}{\bar{n}+2\sqrt{\bar{n}}}\right). \tag{29}$$

The total mean mutual information in this approximation is thus

$$\mathcal{I} = \langle \mathcal{I}_x\rangle + \langle \mathcal{I}_p\rangle \approx \frac{1}{2}\ln\frac{\bar{n}}{4}. \tag{30}$$

The corresponding cost of signal processing (feedforward) has the lower bound [62]

$$E_F \geqslant k_B T_D \frac{1}{2}\ln\frac{\bar{n}}{4}. \tag{31}$$

Therefore, the bound on the cost of feedforward is much lower for large $\bar{n}$ compared to the work gain that scales with $\bar{n}$. One can further lower the cost by reducing the environment temperature T_D.

C. Resetting cost following photocount of entire thermal input

The increase in detector entropy discussed in Sec. II A sets a bound on WOF efficiency by photocount of the entire thermal input

$$\eta \leqslant \frac{\hbar\omega\bar{n} - k_B T_D I_D}{\hbar\omega\bar{n}}. \tag{32}$$

Here the average information stored in the detector that needs to be erased after WOF is

$$I_D = -\sum_m p_m \ln(p_m). \tag{33}$$

For $\bar{n} \gg 1$, this bound becomes

$$\eta \leqslant 1 - \frac{k_B T_D[1+\ln(\bar{n})]}{\hbar\omega\bar{n}}. \tag{34}$$

The condition for nonzero WOF efficiency in this scheme is thus

$$k_B T_D \leqslant \frac{\hbar\omega\bar{n}}{1+\ln(\bar{n})}. \tag{35}$$

This bound on T_D will be compared in what follows to its counterpart by small-fraction WOF. The above bound for nonzero efficiency can also be expressed as

$$\bar{n} \geqslant \bar{n}_D + \frac{1}{1 - \frac{\ln \bar{n}_D}{\ln(\bar{n}_D+1)}}, \tag{36}$$

where $\bar{n}_D$ is the mean number of quanta in the detector when it is kept in an environment at a temperature T_D.

D. Resetting cost for small-fraction photocount WOF

For the small-fraction photocount scheme in Sec. II B, the tradeoff between the detection cost (energy and entropy) and the amount of extracted work obviously depends on the reflected fraction $1-\kappa^2$. Inspired by the optimization for homodyne WOF (Appendix E), we choose the reflected $1-\kappa^2$ fraction to be

$$1-\kappa^2 = 1/\sqrt{\bar{n}}. \tag{37}$$

In this case, the detector uses (absorbs, in the case of photons) $\sqrt{\bar{n}}$ mean quanta for detection, instead of $\bar{n}$ without BS. The mean energy used for detection is $1/\sqrt{\bar{n}}$ fraction of the input. The entropy increase of the detector is given for $\bar{n} \gg 1$ by

$$I_D = 1 + \ln(\sqrt{\bar{n}}). \tag{38}$$

Therefore, the detector heat-up cost is then

$$Q_D = k_B T_D[1 + \ln(\sqrt{\bar{n}})] \tag{39}$$

for large $\bar{n}$. The corresponding upper bound of WOF efficiency is

$$\eta \leqslant \frac{(1 - 1/\sqrt{\bar{n}})\hbar\omega\bar{n} - k_B T_D[1 + \ln(\sqrt{\bar{n}})]}{\hbar\omega\bar{n}}. \tag{40}$$

Hence, for $\bar{n} \gg 1$ the condition of nonzero WOF efficiency is modified to

$$k_B T_D \lesssim \frac{2\hbar\omega\bar{n}}{2 + \ln(\bar{n})}. \tag{41}$$

Therefore, by resorting to the small fraction photocount in Sec. II B, we can almost *double the upper limit* on T_D for work extraction, which is a considerable advantage.

E. Resetting cost for small-fraction homodyne WOF

In this scheme, the entropy increase of the detectors factorizes for x and p, yielding

$$I_{Dx} = I_{Dp} = -\int P(\Delta n_x) \ln P(\Delta n_x) = \frac{1}{2}\left[1 + \ln\left(2\pi\sigma^2_{\Delta n}\right)\right], \tag{42}$$

where

$$P(\Delta n_x, \Delta n_p) \approx \frac{1}{2\pi\sigma^2_{\Delta n}} \exp\left[-\frac{\Delta n_x^2 + \Delta n_p^2}{2\sigma^2_{\Delta n}}\right],$$
$$2\sigma^2_{\Delta n} = 2\beta^2 + \bar{n}(1-\kappa^2)(2\beta^2+1) \approx \bar{n} + 2\sqrt{\bar{n}}. \tag{43}$$

The total entropy increase is then

$$I_D = 2I_{Dx} = 1 + \ln\left(2\pi\sigma^2_{\Delta n}\right) \tag{44}$$

$$= 1 + \ln\pi(\bar{n} + 2\sqrt{\bar{n}}). \tag{45}$$

Therefore, by following the same procedure as for the photocount scheme, we find the upper bound on T_D for nonzero WOF efficiency to be

$$k_B T_D < \frac{\hbar\omega\bar{n}}{1 + \ln(\pi\bar{n})} \tag{46}$$

for $\bar{n} \gg 1$.

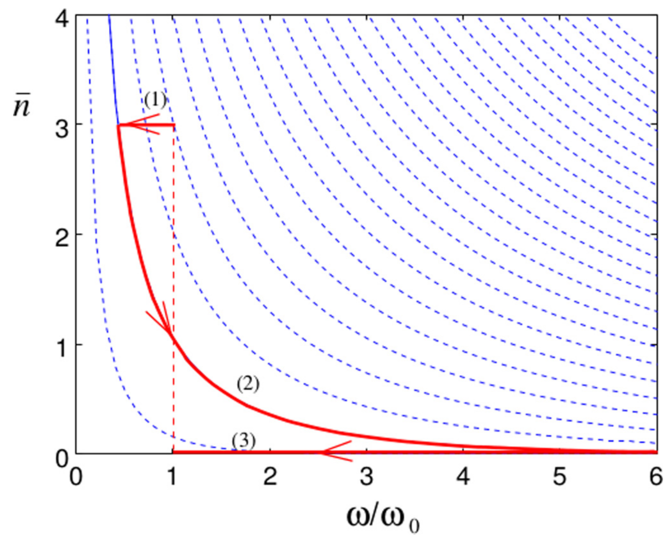

FIG. 7. Resetting the detectors with energy gap $\hbar\omega$ (in units of $\hbar\omega_0$): The evolution is marked by a red line in the $(\omega, \bar{n}_D)$ plane. (1) Starting with $\bar{n}_D = 3$, adiabatically decrease ω to reach the initial temperature. (2) Isothermally increase ω to reach $\bar{n}_D = 0$. (3) Adiabatically return the frequency to its initial value. Broken blue lines are isotherms at various temperatures.

If, instead of small-fraction homodyne one performs homodyning on the entire field, one has

$$P'(\Delta n_x, \Delta n_p) \approx \frac{1}{2\pi\sigma^2} \exp\left[-\frac{\Delta n_x^2 + \Delta n_p^2}{2\sigma^2}\right], \tag{47}$$

where

$$2\sigma^2 = 2\beta^2 + \bar{n}(2\beta^2 + 1) \approx \bar{n}\sqrt{\bar{n}} + \bar{n} + \sqrt{\bar{n}} \tag{48}$$

for large $\bar{n}$. The entropy increase of the detector in this case,

$$I_D = 1 + \ln\pi(\bar{n}\sqrt{\bar{n}} + \bar{n} + \sqrt{\bar{n}}), \tag{49}$$

assuming the same local oscillator energy as for small-fraction homodyning. The upper bound on T_D for nonzero WOF efficiency is then given by

$$k_B T_D < \frac{\hbar\omega\bar{n}}{1 + \ln(\pi\bar{n}^{3/2})} \tag{50}$$

for $\bar{n} \gg 1$. This implies that one can increase the upper bound on T_D almost by a factor of 3/2 by resorting to small-fraction homodyne WOF, instead of the entire field homodyne scheme. If we choose to reduce the environmental temperature of the detector by ΔT_D, the extra invested energy is $\Delta Q_D = C_D\Delta T_D$, where C_D is the heat capacity of the setup.

F. Energetically optimal resetting cost

Let us consider an energetically optimal strategy to reset the photodetectors. A photodetector that consists of N identical two-level atoms that collectively absorb a few quanta may be described by cooperative Dicke states [63–68], which can be approximated for $N \to \infty$ by harmonic-oscillator states. We assume that we can control the detector frequency (energy gap) (see Fig. 7) and implement the following steps:

(i) Adiabatically decrease the frequency ω' of the detector mode until the detector equilibrates with the environment at temperature T_D. This requires

$$\omega' = \frac{k_B T_D}{\hbar} \ln\left(1 + \frac{1}{\bar{n}_D}\right). \tag{51}$$

During this step one can get work in the following amount from the four detectors in homodyne WOF,

$$\begin{aligned} W_1 &= 4\hbar(\omega - \omega')\bar{n}_D \\ &= 4\hbar\omega\bar{n}_D - 4kT_D\bar{n}_D[\ln(\bar{n}_D + 1) - \ln \bar{n}_D]. \end{aligned} \tag{52}$$

(ii) Isothermally increase their frequency to such a value that the mean photon number in the mode vanishes, i.e., $\hbar\omega_f \gg k_B T_D$. To this end, one has to perform the work

$$\begin{aligned} W_2 &= 4\hbar\omega' \frac{\ln(1 + \bar{n}_D)}{\ln\left(1 + \frac{1}{\bar{n}_D}\right)} \\ &= 4k_B T_D \ln(1 + \bar{n}_D). \end{aligned} \tag{53}$$

The heat dissipated to the environment by the four detectors is then

$$\begin{aligned} Q_D &= 4\hbar\omega' \left[\bar{n}_D + \frac{\ln(1 + \bar{n}_D)}{\ln\left(1 + \frac{1}{\bar{n}_D}\right)}\right] \\ &= 4k_B T_D \left[\bar{n}_D \ln\left(1 + \frac{1}{\bar{n}_D}\right) + \ln(1 + \bar{n}_D)\right] \\ &= 4k_B T_D[(\bar{n}_D + 1)\ln(\bar{n}_D + 1) - \bar{n}_D \ln \bar{n}_D]. \end{aligned} \tag{54}$$

(iii) Adiabatically bring the frequency of the oscillator to its initial value. Since no quanta are present at this stage, this action requires no work.

Thus, the work required for resetting the detectors is

$$\begin{aligned} W_{\mathrm{R}} &= W_2 - W_1 \\ &= 4k_B T_D[(\bar{n}_D + 1)\ln(\bar{n}_D + 1) - \bar{n}_D \ln \bar{n}_D] - 4\hbar\omega\bar{n}_D. \end{aligned} \tag{55}$$

From Eqs. (54) and (56), we have

$$Q_D = 4\hbar\omega\bar{n}_D + W_R. \tag{56}$$

Equation (56) shows that the heat dissipated by the detector resetting is partly covered by the energy stored in the detectors, $4\hbar\omega\bar{n}_D$, and partly by additional work, W_R, that needs to be invested in the resetting. This additional work can, however, be zero for $\bar{n}_D$ satisfying

$$\frac{\hbar\omega}{k_B T_D} = \left(1 + \frac{1}{\bar{n}_D}\right)\ln(\bar{n}_D + 1) - \ln \bar{n}_D. \tag{57}$$

For $\bar{n}_D$ higher than this value, the net work W_{R} is negative. Namely, one can get useful work by resetting the detectors to zero by manipulating the detector frequency.

While the outlined method may, in principle, save us energy or work on the detector resetting, it suffers from some drawbacks. It is adiabatic, i.e., extremely slow, and requires frequency manipulation of the detectors modeled as oscillators. Yet, it is preferable to reset the detectors by continuously cooling them at the highest rate possible, since the work consumption is modest provided the initial detector temperature is low enough. It is particularly important to maximize the WOF power, which is limited by the detector cooling time. State-of-the-art superconducting photodetection allows ns-scale detector resetting by cooling [69,70].

IV. WORK EXTRACTION FROM PARTIAL INFORMATION: COARSE-GRAINING EFFECTS

A. Why consider coarse-graining?

For practical reasons, detectors may not have sufficient resolution to record the full information available on the input state, either by photocounts or homodyning. This situation prompts a conceptual question: how does the tradeoff between resolution and information affect the extractable work efficiency?

The distribution of photocounts in each detector, for large quanta numbers, can be well approximated by the Gaussian distribution. The question is, how does this distribution change under coarse-graining? The Gaussian distribution of a random variable x has the form $G(x) = \frac{1}{\sigma\sqrt{2\pi}} e^{-\frac{1}{2}(\frac{x-\mu}{\sigma})^2}$. We take, as is customary, the continuous limit of the photocount probability function (although the counts are discrete). We assume the coarse-grained detector to be such that it cannot differentiate between counts of photocounts in blocks of size R. We set the blocks such that the mean of the distribution is in the middle of a block. As an example, The probability that an outcome is in a block which is, say, M blocks to the right from the mean is given by

$$\int_{r1}^{r2} G(x)dx = \pi\left(\mathrm{Erf}\left[\frac{\mu - r_1}{\sqrt{2}\sigma}\right] - \mathrm{Erf}\left[\frac{\mu - r_2}{\sqrt{2}\sigma}\right]\right), \tag{58}$$

where $r_1 = \mu + (M + 1/2)R$, $r_2 = \mu + (M + 3/2)R$ and the error function $\mathrm{Erf}(x) = \int_0^x e^{-t^2} dt$. The protocol is then as follows:

(i) Assume the resolution of the detectors is R; for the $\Delta n_{x/p}$ records assume the values $0, R, 2R, \ldots, NR$.

(ii) Calculate the average postmeasured state and the corresponding work extractable by displacement from each block of area $R \times R$ to get the average work gain from the coarse-grained WOF.

B. Extremely coarse grained homodyning: WOF via sign measurements

Let us consider an extreme coarse-grained situation in which the detected signal (Δn_x or Δn_p) is positive (+) or negative (−). There are four distinct possibilities for $\mathrm{sgn}(\Delta n_x)$ and $\mathrm{sgn}(\Delta n_p)$, corresponding to work gain by displacement $W_{++}, W_{+-}, W_{-+}, W_{--}$: For, e.g., W_{+-} we get

$$W_{+-} = \frac{\hbar\omega}{2}(\langle\hat{x}\rangle_{+-}^2 + \langle\hat{p}\rangle_{+-}^2) = \hbar\omega\frac{\kappa^2}{16\gamma^2}\frac{2\sigma_{\Delta n}^2}{\pi}. \tag{59}$$

Here we have used

$$\begin{aligned} \langle\hat{x}\rangle_{+-} &= \kappa \int_{-\infty}^{-\infty} dx \int_{-\infty}^{-\infty} dp \int_{-\infty}^{0} d\Delta n_p \int_{0}^{\infty} d\Delta n_x \\ &\quad \times xP(x, p|\Delta n_x, \Delta n_p)P(\Delta n_x, \Delta n_p) \\ &= \frac{\kappa}{4\gamma}\sqrt{\frac{2\sigma_{\Delta n}^2}{\pi}}, \end{aligned}$$

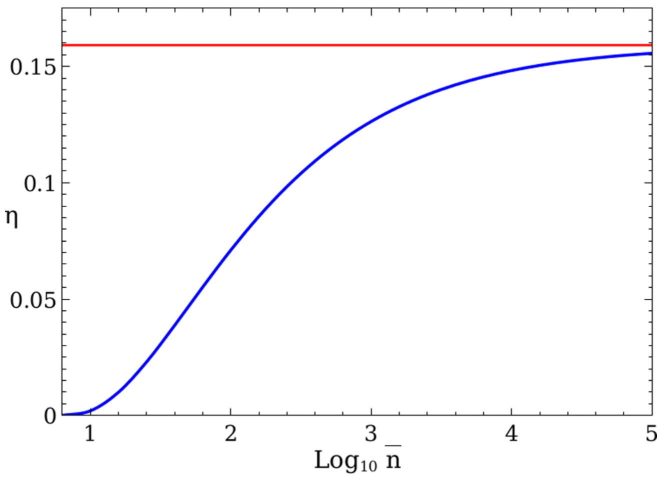

FIG. 8. Efficiency $\eta = W/\hbar\omega\bar{n}$ plotted vs the mean number of input quanta $\bar{n}$ for the scheme of sign measurement WOF. The red line represents the maximal $\eta = 1/2\pi$.

$$\langle\hat{p}\rangle_{+-} = -\frac{\kappa}{4\gamma}\sqrt{\frac{2\sigma_{\Delta n}^2}{\pi}},$$
$$\gamma = \beta\sqrt{1-\kappa^2}\left[1 + \frac{1}{\bar{n}(1-\kappa^2)} + \frac{1}{2\beta^2}\right],$$
$$\sigma_{\Delta n}^2 = \beta^2 + \bar{n}(1-\kappa^2)\left(\beta^2 + \frac{1}{2}\right). \quad (60)$$

The total average work obtained by downshifting the postmeasured state following a sign measurement is evaluated to be

$$\begin{aligned} W &= W_{++} + W_{+-} + W_{-+} + W_{--} - W_{\mathrm{LO}} \\ &= \hbar\omega\frac{\kappa^2}{4\gamma^2}\frac{2\sigma_{\Delta n}^2}{\pi} - 2\hbar\omega\beta^2 \\ &= \frac{\hbar\omega}{2\pi}\frac{2\beta^2\kappa^2(1-\kappa^2)\bar{n}^2}{2\beta^2 + (1-\kappa^2)(1+2\beta^2)\bar{n}} - 2\hbar\omega\beta^2. \end{aligned} \quad (61)$$

The positive part (work gain) of Eq. (61) is similar to its counterpart Eq. (52) for the work gain by fine-grained homodyning, but in Eq. (61) the work is smaller by a factor of $\frac{1}{2\pi}$, since the phase is not recorded by sign measurement.

The minimum mean number of quanta for nonzero efficiency by sign measurement is $\bar{n} = 2\pi$ as opposed to $\bar{n} = 1$ for fine-grained homodyne WOF. For large $\bar{n}$, W is optimized when $2\beta^2 \approx \sqrt{\frac{\bar{n}}{2\pi}}$ and $1-\kappa^2 \approx \frac{1}{\sqrt{\bar{n}}}$, the extractable work then being

$$W \approx \frac{\hbar\omega}{2\pi}\left[\bar{n} - 2(1+\sqrt{2\pi})\sqrt{\bar{n}} + 1 + \sqrt{2\pi} + O\left(\frac{1}{\sqrt{\bar{n}}}, \frac{1}{\bar{n}}\right)\right]. \quad (62)$$

The efficiency of this scheme is bounded by $\frac{1}{2\pi}$ (see Fig. 8).

The mutual information gain by sign measurement is given by (Appendix F)

$$\mathcal{I} = -\iint P(x,p)S(p(a,b|x,y))dx\,dp + S(p(a,b)), \quad (63)$$

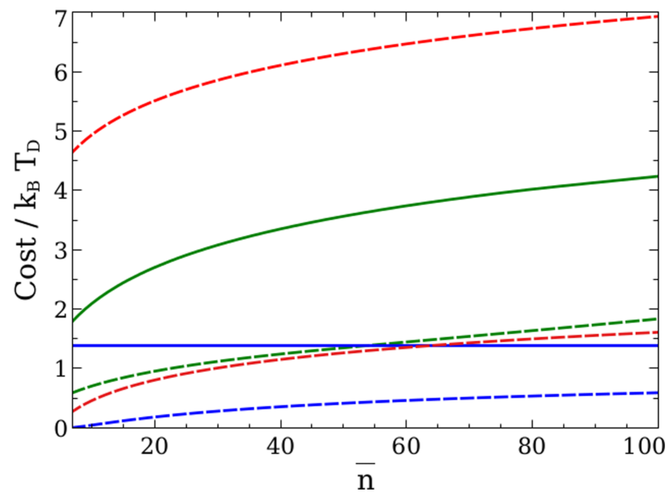

FIG. 9. The cost of erasing the detector information (solid lines) after the completion of WOF [Eqs. (44), (33), and (64)] and feedforward (dashed lines) [Eqs. (30), (25), and (63)] are plotted upon normalization by k_BT_D, where T_D is the environment temperature at which the detector is kept. The red, green, and blue correspond to the small-fraction homodyne, photocount, and sign WOF schemes, respectively. For small-fraction photocount, BS transmissivity $\kappa^2 = 0.75$ has been considered. Clearly, Q_D, $E_F \ll W$ for $\hbar\omega = k_BT_D$.

where $a, b \in \{+,-\}$. Here the entropy gain by the detectors for the sign measurement is $S(p(a,b)) = \ln 4$, i.e.,

$$I_D = \ln 4. \quad (64)$$

This mutual information is evaluated by taking the logarithm of the probabilities,

$$\begin{aligned} p(+,-|\alpha) &= \int_0^\infty\int_{-\infty}^0 P(\Delta n_x, \Delta n_p|\alpha)d\Delta n_x d\Delta n_p \\ &= \frac{1}{4}\left(1 + \mathrm{Erf}\left[\frac{\mu_x}{\sqrt{2}\sigma_\alpha}\right]\right)\left(1 - \mathrm{Erf}\left[\frac{\mu_p}{\sqrt{2}\sigma_\alpha}\right]\right), \end{aligned} \quad (65)$$

where $\mu_x = \sqrt{2(1-\kappa^2)}\beta\,\mathrm{Re}\alpha$, $\mu_p = \sqrt{2(1-\kappa^2)}\beta\,\mathrm{Im}\alpha$, and $\sigma_\alpha = [\frac{(1-\kappa^2)|\alpha|^2}{2} + \beta^2]^{1/2}$.

Similarly,

$$\begin{aligned} p(+,+|\alpha) &= \frac{1}{4}\left(1 + \mathrm{Erf}\left[\frac{\mu_x}{\sqrt{2}\sigma_\alpha}\right]\right)\left(1 + \mathrm{Erf}\left[\frac{\mu_p}{\sqrt{2}\sigma_\alpha}\right]\right), \\ p(-,+|\alpha) &= \frac{1}{4}\left[\left(1 - \mathrm{Erf}\left[\frac{\mu_x}{\sqrt{2}\sigma_\alpha}\right]\right)\left(1 + \mathrm{Erf}\left[\frac{\mu_p}{\sqrt{2}\sigma_\alpha}\right]\right)\right., \\ p(-,-|\alpha) &= \frac{1}{4}\left(1 - \mathrm{Erf}\left[\frac{\mu_x}{\sqrt{2}\sigma_\alpha}\right]\right)\left(1 - \mathrm{Erf}\left[\frac{\mu_p}{\sqrt{2}\sigma_\alpha}\right]\right). \end{aligned} \quad (66)$$

We find numerically that the lower bound of feedforward cost, $E_F \geqslant k_BT_D\mathcal{I}$, is much lower compared to the fine-grained homodyne case (see Fig. 9).

These results for work extraction from sign measurements may be compared to those of the recently proposed Szilard/Maxwell Demon binary measurement engines [45]: a scheme where two thermal fields with $\bar{n}$ photons each are incident on two highly transmitting BS. A photon click or no-click is registered for the reflected part in two detectors resulting in two bits of information at most. If a detector clicks with probability $1/2$, then $\bar{n}$ of the corresponding output field increases to $(3/2)\bar{n}$. For no click, the mean decreases to $(1/2)\bar{n}$. Only events where one detector clicks and the other one does not (in 50% of the cases) produce a net photocurrent that charges a capacitor, with $(1/2)\bar{n}$ photons convertible to photocurrent. Since the two beams have in total $2\bar{n}$, only $1/4$ of the input energy contributes to work, so that the efficiency bound is $1/4$. Optimization of the click probabilities yields an efficiency bound to ~ 0.3 as compared to near-unity efficiency for $\bar{n} \gg 1$ by our small-fraction homodyne WOF in Sec. II C.

The comparison of the efficiency bound obtained by such binary methods with fine-grained WOF shows the clear superiority of the latter. In contrast, the sign measurement provides comparable performance to Maxwell-Demon binary measurement engines.

V. CAN NONSELECTIVE MEASUREMENTS YIELD WORK?

Since WOF relies on selective measurements that provide mutual information on the input state, a basic question is whether NSMs, which do not provide mutual information, can yield work. In Sec. V A we show that NSMs are indeed useless for WOF. By contrast, in Sec. V B we show that NSMs in a basis that does not commute with the Hamiltonian can yield not only heat (as shown in Ref. [71]), but also ergotropy. Finally, in Sec. V C we show that NSMs of correlated modes can also yield work.

A. NSM of a small fraction: No work

Consider an arbitrary generalized positive operator valued measurement (POVM), represented by Kraus operators $K_i^\dagger K_i$ for different outcome i, that satisfies $\sum_i K_i^\dagger K_i = \mathcal{I}$, where $\mathcal{I}$ denotes the identity operator [61]. If we measure the reflected part (see Fig. 4) and find the ith outcome corresponding to the Kraus operator $K_i^\dagger K_i$, then the postmeasured transmitted state is given by

$$\rho(i) = \int\int \frac{p(i|\alpha)P(\alpha)}{p(i)} |\kappa\alpha\rangle\langle\kappa\alpha| d^2\alpha, \tag{67}$$

where $p(i|\alpha) = \mathrm{Tr}[K_i^\dagger K_i |\alpha\rangle\langle\alpha|]$. Therefore, the postmeasured state for NSM state is

$$\begin{aligned}\rho(\mathrm{NSM}) &= \int\int \sum_i p(i) \frac{p(i|\alpha)P(\alpha)}{p(i)} |\kappa\alpha\rangle\langle\kappa\alpha| d^2\alpha \\ &= \int\int P(\alpha)|\kappa\alpha\rangle\langle\kappa\alpha| d^2\alpha \\ &= \frac{1}{\kappa^2}\int\int P(\frac{\alpha}{\kappa})|\alpha\rangle\langle\alpha| d^2\alpha. \end{aligned} \tag{68}$$

This holds true for any complete set of measurements, as

$$\sum_i p(i|\alpha) = \mathrm{Tr}\left[\sum_i K_i^\dagger K_i |\alpha\rangle\langle\alpha|\right] = \mathrm{Tr}[\mathcal{I}|\alpha\rangle\langle\alpha|] = 1 \tag{69}$$

using the linearity of the trace. From Eq. (68), we see that the form of the input P-distribution remains unaltered for NSM, and thus the distribution remains thermal with modified mean quanta $\bar{n} \to \kappa^2\bar{n}$. Therefore, NSM is a no-go strategy for WOF, where feedforward of the measurement result is essential.

B. NSM in a noncommuting basis with the Hamiltonian: Heat and ergotropy

If we perform a NSM in a basis $\{|i\rangle\}$ that does not commute with an energy basis, the state becomes diagonal in this basis,

$$\rho_{\mathrm{NSM}} = \sum_i p_i |i\rangle\langle i|. \tag{70}$$

Since this basis is off-diagonal in energy eigenbasis,

$$|i\rangle = \sum_n c_{n,i}|E_n\rangle, \tag{71}$$

where $|E_n\rangle$'s are the energy eigenstate. Therefore, the postmeasured state following a NSM in a basis that is noncommuting with H ($[\rho_{\mathrm{NSM}}, H] \neq 0$) is nonpassive, since a passive state is always diagonal in an energy basis (Appendix A).

In [71], the authors showed that work can be extracted from a single-temperature thermal resource and measurement without feedforward in a four-stroke engine by a protocol, which we modify here to account for the possible nonpassivity of the postmeasured state:

(i) The system, which is initially in equilibrium with a heat bath at temperature T [and thus in a diagonal state in the energy basis $\rho_I(\lambda_i) = \sum_n p_n^{\mathrm{eq}}(\lambda_i)|E_n\rangle\langle E_n|$], undergoes an adiabatic transformation by changing its energy level spacings from λ_i to λ_f without changing the population. Work is thereby done on the system, in the amount

$$W_I = \sum_n [E_n(\lambda_f) - E_n(\lambda_i)] p_n^{\mathrm{eq}}(\lambda_i). \tag{72}$$

(ii) The system is then measured in a basis other than the energy eigenbasis: While keeping the Hamiltonian $H(\lambda_f)$ fixed, an impulsive measurement with possible outcomes M_j, $j = 1 \to N$, of an observable that does not commute with $H(\lambda_f)$ is performed on the system. This state change implies a change of the occupation probabilities of the energy eigenstates:

$$\rho_I(\lambda_f) \to \rho_{\mathrm{NSM}} = \sum_j M_j^\dagger \rho_I(\lambda_f) M_j. \tag{73}$$

This measurement acts as a hot bath that imparts heat into the system in the amount

$$Q_M = \sum_{m,n} [E_m(\lambda_f) - E_n(\lambda_f)] T_{mn} p_n^{\mathrm{eq}}(\lambda_i), \tag{74}$$

where $T_{mn} = \sum_j |\langle E_m|M_j|E_n\rangle|^2$ denotes the transition probability from $|E_n\rangle$ to $|E_m\rangle$. One can view the heat Q_M to be provided by a hot bath at temperature T_M.

As opposed to Ref. [71], we find that the NSM can yield not only heat but also ergotropy, $\Delta\mathcal{W}_{\mathrm{NSM}}$, whose upper bound can be obtained as

$$\Delta\mathcal{W}_{\mathrm{NSM}} \leqslant E(\rho_{\mathrm{NSM}}) - E(\rho_{T'}), \tag{75}$$

where $\rho_{T'}$ is a thermal state with Hamiltonian $H(\lambda_f)$ at temperature T', such that $S(\rho_{\mathrm{NSM}}) = S(\rho_{T'})$. Thus, in contrast to a four-stroke engine, where a hot bath renders the system in a higher energy but still passive state, such an NSM can change the character of the energy state distribution.

(iii) In the second adiabatic step, the parameter changes from λ_f back to the initial value λ_i. The work done by the system is then given by

$$W_{\mathrm{II}} = \sum_n [E_n(\lambda_i) - E_n(\lambda_f)]p_n^{\mathrm{NSM}}, \tag{76}$$

where p_n^{NSM}, the probability of finding the nth eigenstate in the postmeasurement state [Eq. (73)], is given by

$$p_n^{\mathrm{NSM}} \equiv \langle n;\lambda|\rho_{\mathrm{NSM}}|n;\lambda\rangle. \tag{77}$$

(iv) The final step is thermalization with a cold bath at temperature T_c.

The efficiency of this scheme in Ref. [71] is given by

$$\eta = \frac{-(W_{\mathrm{I}} + W_{\mathrm{II}})}{Q_M}. \tag{78}$$

As noted above, the treatment in Ref. [71] has not allowed for the possibility that the measurement may also impart ergotropy $\Delta\mathcal{W}_{\mathrm{NSM}}$ to the system, as does a nonpassive (e.g., squeezed) bath [25]. The appropriate efficiency bound then becomes

$$\eta_{\max} \leqslant 1 - \frac{T_c}{T_M}\frac{Q_M}{Q_M + \Delta\mathcal{W}_{\mathrm{NSM}}}, \tag{79}$$

which can be evaluated by Eq. (75). This efficiency may *exceed the Carnot bound*, thus proving that this machine is not a heat engine.

C. NSM in a mode-correlated cycle

Here we consider work via NSM from two oscillator modes, hot (h) and cold (c), that are correlated by their interaction, unlike the input modes in Sec. II. Let us consider a brief QND measurement that decorrelates modes, thus altering their correlation energy. Subsequent periodic modulation of the modes frequencies allows for work extraction following *an impulsive* measurement by a detector D. The total Hamiltonian describing a system consisting of two (hot-h and cold-c) interacting modes described by the Hamiltonian $H_S = H_h + H_c + H_{hc}$ and a detector is

$$H_{\mathrm{tot}} = H_{\mathrm{S}} + H_{\mathrm{SD}}, \tag{80}$$

where H_{SD} is the impulsive system-detector interaction that does not commute with H_{S} ($[H_{\mathrm{S}}, H_{\mathrm{SD}}] \neq 0$). This total Hamiltonian is assumed to be τ-periodic, $H_{\mathrm{tot}}(\tau) = H_{\mathrm{tot}}(0)$. Work extraction comes about because the NSM changes the intermode mean correlation energy $\langle H_{hc}\rangle$.

When the detector is traced out, the entropy and energy of the single mode change since the NSM decorrelates the modes, thereby increasing their correlation energy by

$$\Delta E_{\mathrm{D}} = -\langle H_{hc}\rangle_{\mathrm{Eq}} \; > 0. \tag{81}$$

This scenario stands in contrast to Landauer's [42], where such correlations are not accounted for. If the cycle duration is shorter than the correlation time, $t_{\mathrm{cycle}} < t_c$, but longer than the time needed to perform the measurement, the maximal amount of extractable work, without measurement readout (for an NSM), is given by

$$(W_{\mathrm{NSM}})_{\max} = \Delta E_{\mathrm{D}} - T_D\Delta\mathcal{S}_{\mathrm{D}}, \tag{82}$$

where $\Delta\mathcal{S}_{\mathrm{D}}$ is the entropy increase of the detector due to the NSM.

The energy ΔE_{D} consumed by the detector can be a thermal noisy pulse, described by a passive state, so that neither the detector nor these modes can store ergotropy. The NSM-based cycle converts such passive input into a nonpassive output state capable of delivering work.

Such a cycle exemplifies the conclusion that, upon entangling the initially uncorrelated passive (but nonthermal) states of distinct subsystems, here the intermode and the detector, the state of one subsystem (here the hot mode) may become nonpassive and thus deliver work.

The maximum work (per cycle) extractable from a selective measurement, $(W_{\mathrm{sel}})_{\max}$, clearly exceeds the NSM-work, $(W_{\mathrm{NSM}})_{\max}$:

$$(W_{\mathrm{sel}})_{\max} = (W_{\mathrm{NSM}})_{\max} + W, \tag{83}$$

where W is the work obtained by WOF in Sec. II or IV in the absence of ΔE_D. The extra work $(W_{\mathrm{NSM}})_{\max}$ stems from correlations or entanglement unaccounted for by the Landauer principle.

Remarkably, an NSM in this scenario allows for work extraction from a bath at $T_D = 0$, without information gain: The reason is that the correlation energy is always negative, even at $T_D = 0$. Hence, decorrelation of the modes through a measurement increases the total energy allowing the cycle to be triggered, yielding the extractable work

$$(W_{\mathrm{sel}})_{\max} = (W_{\mathrm{NSM}})_{\max} > 0. \tag{84}$$

A similar situation arises for a system and a bath that adhere to the spin-boson model [72], where work extraction via NSM can only take place within the correlation timescales. The joint, entangled multimode state initially at equilibrium, ρ_{eq}, is changed [73] to a product state by the impulsive NSM [72,73].

VI. CONCLUSIONS

Our comparative analysis of heat to work conversion in few-mode setups by measurements has led to the following findings:

(A) As compared to the previously proposed work extraction by measuring a variable of the entire input [45], we have shown (Sec. II) that it is advantageous to measure only a small fraction of the input and extract work from the dominant, unmeasured fraction by generalizing our recently proposed method of work by observation and feedforward (WOF) [57]. The main advantage of measuring a small fraction, either by photocount or by homodyning, is that it bears a much smaller cost in terms of information (entropy) consumed by feedforward and by resetting the detectors (after WOF has been completed).

(B) We have argued (Sec. III) that, practically, the resetting of the detectors should preferably be done as fast as possible, since detector cooling to its initial temperature may carry a modest energy and entropy cost compared to the extracted work.

(C) Measurements with partial resolution (coarse-graining) have been shown (Sec. IV) to yield much less information as well as work and efficiency than their fine-graining counterparts, thereby establishing the rapport of work and information extraction. Yet, WOF based on extreme coarse-graining of a small fraction has been shown to favorably compare with binary-measurement (Maxwell-demon) information machines [45–48].

(D) Finally, unread or nonselective measurements (NSMs) [2] have been shown (Sec. V) to yield no work when applied in WOF. Yet, they may extract work when performed in a basis that does not commute with the Hamiltonian: In fact, we have shown that NSMs may yield considerably more work than previously proposed [71,74]. In scenarios in which the modes are nonlinearly correlated, NSM has been noted to yield work from the intermode correlation energy, a consideration absent in Landauer's principle [42]. These scenarios are analogous to work extraction by NSM from system-bath correlations in the non-Markovian time domain [72].

The present analysis has not only conceptual but also practical merit, in particular for optical setups and their acoustic counterparts. While the *spatial profile* of electromagnetic or acoustic field propagation and its mode decomposition are well controlled by simple elements (collimators, beam splitters, lenses, etc.), *temporal fluctuations* are much harder to control. Our comparative analysis has presented guidelines to the alternative methods by which such control can be accomplished for single-mode, i.e., spatially well-collimated propagation of thermal noise, resulting in optimized work extraction. The bounds on this work extraction and the corresponding power have been quantified by the minimal costs required for these tasks, i.e., information transfer for feedforward and detector resetting.

These bounds are important for determining the feasibility of few-quanta conversion from heat to work. Optical elements have been shown to allow the increased concentration of sunlight so that the stationary power that arrives at the detector on average is multiphoton, but it has thus far been unclear what level of power suffices for work generation. Our analysis makes us cautiously optimistic that this task may be experimentally accomplished with a few photons. It may manifest itself, e.g., as the transformation of concentrated sunlight input into nearly coherent or number-squeezed light at the output and thereby produce reduced quantum fluctuations in an optomechanical device [54]. Alternatively, thermal light input may yield low-noise (low-entropy) photocurrent [58,75] that can be instrumental for quantum operation of electronic devices.

The WOF protocols for work extraction discussed in Secs. II and IV are not only applicable to optical systems, but also to any noisy source, where homodyning or quanta number count of continuous variables can be performed. For example, in ultracold bosonic gases, homodyning was proposed [76] and demonstrated [77]. Photocurrents induced by signal-pump interference in semiconductors [75,78] and phonon fields in acoustic structures [79–83] also allow to split off a small fraction of the input field for observation (homodyning or others), thereby yielding work from the dominant part of the input. Thus, the proposed WOF schemes may pave the way towards work extraction in both classical and quantum regimes of diverse systems using continuous-variable noise as a resource.

ACKNOWLEDGMENTS

A.M. thanks Arnab Chakrabarti, Nilakantha Meher, and Saikat Sur of WIS for useful discussions. T.O. is supported by the Czech Science Foundation, Grant No. 20-27994S. G.K. is supported by DFG (FOR 2724), QUANTERA (PACE-IN), and NSF-BSF.

APPENDIX A: ERGOTROPY AND WORK EXTRACTION

At the outset, we briefly present the key expressions for work and heat extractable from a quantum system. These expressions can help guide us through the different work extraction processes in Secs. II–V.

Ergotropy is the maximum amount of work extractable for a given Hamiltonian H from a state ρ with mean energy $\langle E\rangle$ by unitary transformations. It is quantified as [7,8,25,49–51,53]

$$\mathcal{W}(\rho, H) \equiv \mathrm{Tr}(\rho H) - \min_{U} \mathrm{Tr}(U\rho U^{\dagger} H) \geqslant 0, \tag{A1}$$

where the minimization encompasses all possible unitary transformations U. To have $\mathcal{W}(\rho, H) > 0$, the state ρ must be nonpassive, i.e., it must correspond to a *nonmonotonic or anisotropic* distribution of energy eigenvalues (Figs. 3 and 5). The mean energy $\langle E\rangle$ of such a state ρ can be divided into ergotropy $\mathcal{W}$ and passive energy, i.e., the energy that cannot be extracted as useful work by a unitary operation, which is given by

$$\langle E\rangle - \mathcal{W} = \mathrm{Tr}(U_{\mathrm{p}}\rho U_{\mathrm{p}}^{\dagger} H) = \mathrm{Tr}(\Pi H). \tag{A2}$$

Here U_{p} is the unitary transformation from state ρ to its (unique) passive counterpart state Π. This transformation minimizes the second term on the right-hand side of (A1).

The ergotropy may increase in a nonunitary fashion due to the interaction of the system with a bath and be subsequently extracted as work via a unitary process. Any *unitary* change in the passive energy of a system driven by a time-dependent Hamiltonian results in a change in the extracted work. The ergotropy of a quantum state may change as a result of a measurement. In this article, the measurement-based WOF protocols render a passive (thermal) state nonpassive, i.e., endow it with ergotropy.

In the case of small-fraction homodyne WOF, as the distribution is displaced from the origin, the ergotropy can be extracted by displacement (downshift) of the state ρ to the origin [57],

$$\Delta\mathcal{W} = \frac{\hbar\omega}{2}(\langle\hat{x}\rangle^2 + \langle\hat{p}\rangle^2), \tag{A3}$$

where $\langle\hat{x}\rangle$ and $\langle\hat{p}\rangle$ are the mean values of the position and the momentum, respectively.

In the case of small-fraction photocount, nonpassivity is manifested by the nonmonotonic occupation probabilities of the number states (see Fig. 2). In this case, work can be extracted from the postmeasured state by permutation of the number-state basis.

APPENDIX B: THERMODYNAMICS OF A SINGLE OSCILLATOR MODE

Starting from the partition function

$$Z = \sum_{n=0}^{\infty} \exp\left(-\frac{\hbar\omega}{k_B T} n\right) = \frac{1}{1 - \exp\left(-\frac{\hbar\omega}{k_B T}\right)} = \frac{1}{1 - \exp(-\beta\hbar\omega)}, \tag{B1}$$

one finds the mean energy

$$E = \frac{1}{Z}\frac{\partial Z}{\partial(1/k_B T)} = \frac{\hbar\omega}{\exp\left(\frac{\hbar\omega}{kT}\right) - 1} = \hbar\omega\bar{n}. \tag{B2}$$

Expressing the relationship between temperature and mean photon number as

$$T = \frac{\hbar\omega}{k_B \ln\left(1 + \frac{1}{\bar{n}}\right)}, \tag{B3}$$

we can express the partition function as

$$Z = \bar{n} + 1, \tag{B4}$$

entropy as

$$S = k_B(\ln Z + E/k_B T) = k_B[(\bar{n}+1)\ln(\bar{n}+1) - \bar{n}\ln\bar{n}], \tag{B5}$$

and free energy as

$$\mathcal{F} = -k_B T \ln Z = -\hbar\omega + k_B T \ln\left[\exp\left(\frac{\hbar\omega}{k_B T}\right) - 1\right] = -\hbar\omega\frac{\ln(1+\bar{n})}{\ln\left(1 + \frac{1}{\bar{n}}\right)}. \tag{B6}$$

We can write the first law (or, more precisely, the combined theorem) of thermodynamics as

$$dE = T dS + \mathcal{P} d\omega, \tag{B7}$$

where $T dS = \hbar\omega d\bar{n}$ is the heat entering the system and $\mathcal{P} d\omega$ is the work done on the system by changing the frequency, where the "pressure" $\mathcal{P}$ is given by the derivative $\mathcal{F}$ with respect to ω,

$$\mathcal{P} = \left(\frac{\partial \mathcal{F}}{\partial \omega}\right)_T = \frac{\hbar}{\exp\left(\frac{\hbar\omega}{kT}\right) - 1} = \hbar\bar{n}. \tag{B8}$$

Thus, we can express the work done on the system as free energy change, and heat entering the system as entropy change during an isothermal process,

$$W = \mathcal{F}_2 - \mathcal{F}_1 = \hbar(\omega_1 - \omega_2) + kT \ln\frac{\exp\left(\frac{\hbar\omega_2}{kT}\right) - 1}{\exp\left(\frac{\hbar\omega_1}{kT}\right) - 1} = \hbar\left[\omega_1\frac{\ln(1+\bar{n}_1)}{\ln\left(1+\frac{1}{\bar{n}_1}\right)} - \omega_2\frac{\ln(1+\bar{n}_2)}{\ln\left(1+\frac{1}{\bar{n}_2}\right)}\right], \tag{B9}$$

$$\begin{aligned} Q &= T(S_2 - S_1) \\ &= \hbar\left[\frac{\omega_2}{\exp\left(\frac{\hbar\omega_2}{kT}\right) - 1} - \frac{\omega_1}{\exp\left(\frac{\hbar\omega_1}{kT}\right) - 1}\right] \\ &\quad + kT \ln\frac{1 - \exp\left(-\frac{\hbar\omega_1}{kT}\right)}{1 - \exp\left(-\frac{\hbar\omega_2}{kT}\right)} \\ &= \hbar\omega_2\frac{(\bar{n}_2+1)\ln(\bar{n}_2+1) - \bar{n}_2\ln\bar{n}_2}{\ln\left(1+\frac{1}{\bar{n}_2}\right)} \\ &\quad - \hbar\omega_1\frac{(\bar{n}_1+1)\ln(\bar{n}_1+1) - \bar{n}_1\ln\bar{n}_1}{\ln\left(1+\frac{1}{\bar{n}_1}\right)}. \end{aligned} \tag{B10}$$

Considering the limit $\hbar\omega_2 \gg k_B T$, one can find the work necessary to isothermally compress the oscillator to infinite ω, as well as the corresponding heat (using here $\bar{n}$ and ω instead of $\bar{n}_1$ and ω_1),

$$W_\infty = -\mathcal{F} = \hbar\omega - k_B T \ln\left[\exp\left(\frac{\hbar\omega}{k_B T}\right) - 1\right] = \hbar\omega\frac{\ln(1+\bar{n})}{\ln\left(1+\frac{1}{\bar{n}}\right)}, \tag{B11}$$

$$Q_\infty = -TS = -\hbar\omega\left[\bar{n} + \frac{\ln(1+\bar{n})}{\ln\left(1+\frac{1}{\bar{n}}\right)}\right]. \tag{B12}$$

As can be seen, $W_\infty + Q_\infty = -\hbar\omega\bar{n}$, i.e., during an isothermal process the work spent on increasing ω plus the initial energy $\hbar\omega\bar{n}$ are converted into heat going to the environment. Note that in the limit $k_B T \gg \hbar\omega$, or $\bar{n} \gg 1$, one gets

$$W_\infty \approx \hbar\omega\left[\left(\bar{n} + \frac{1}{2}\right)\ln\bar{n} + 1\right], \tag{B13}$$

$$Q_\infty \approx -\hbar\omega\left[\left(\bar{n} + \frac{1}{2}\right)\ln\bar{n} + \bar{n} + 1\right]. \tag{B14}$$

APPENDIX C: PHOTOCOUNT OF A REFLECTED THERMAL BEAM

When a Fock state $|n\rangle$ is incident on a beam-splitter (BS) with transmissivity κ^2, the transmitted state [60] is

$$|n, 0\rangle_{\rm out} = \sum_{q=0}^{n}\sqrt{\frac{n!}{(n-q)!q!}}(\kappa)^q\left(\sqrt{1-\kappa^2}\right)^{n-q}|q, n-q\rangle. \tag{C1}$$

If we detect m photons in the reflected beam, the resulting transmitted state is $|n-m\rangle$. This event has the probability

$$p'_m = \frac{n!}{(n-m)!m!}(\kappa^2)^{n-m}(1-\kappa^2)^m. \tag{C2}$$

For a thermal input as in Eq. (5), detecting m quanta in the reflected beam has the probability

$$p_m = \frac{(1-\kappa^2)^m\left(1 - e^{-\frac{\hbar\omega}{k_B T}}\right)e^{-\frac{\hbar\omega}{k_B T}m}}{\left(1 - e^{-\frac{\hbar\omega}{k_B T}}\kappa^2\right)^{(m+1)}}. \tag{C3}$$

As the BS does not change the distribution of the input, the reflected beam corresponds to a thermal distribution with mean quanta number $(1-\kappa^2)\bar{n}$ [Eq. (7)]. The average energy of the postmeasured state is

$$E_m = \hbar\omega\bar{n}_m = \hbar\omega\sum_{n=0}^{\infty} p(n|m)n = \hbar\omega\frac{(1+m)\kappa^2}{e^{\frac{\hbar\omega}{k_B T}}-\kappa^2}. \tag{C4}$$

Assume a thermal state with mean photon number $\bar{n}$ entering a beam splitter with reflectivity

$$R = 1-\kappa^2. \tag{C5}$$

The reduced density matrix for the reflected beam corresponds to a thermal state with mean photon number $R\bar{n}$. Let us assume that m photons in the reflected beam were detected. The conditional probability distribution of the photon number n is evaluated,

$$p(n|m) = \frac{p(n\wedge m)}{p_{\text{refl}}(m)}, \tag{C6}$$

where $p(n\wedge m)$ denotes the joint probability of having m photons in the reflected beam and n photons in the transmitted beam. It is given by

$$p(n\wedge m) = p(n\wedge m|n+m)p_{\text{in}}(n+m), \tag{C7}$$

$$p(n\wedge m|n+m) = \binom{n+m}{m}R^m(1-R)^n, \tag{C8}$$

$$p_{\text{in}}(n+m) = \frac{\bar{n}^{n+m}}{(\bar{n}+1)^{n+m+1}}, \tag{C9}$$

$$p_{\text{refl}}(m) = \frac{(R\bar{n})^m}{(R\bar{n}+1)^{m+1}}, \tag{C10}$$

where $p_R(m)$ is the marginal probability of having m photons in the reflected beam, and $p_{\text{in}}(n+m)$ is the probability of having $n+m$ photons in the incoming beam. Using these equations, one finds

$$\begin{aligned} p(n|m) &= \binom{n+m}{m}R^m(1-R)^n\frac{\bar{n}^{n+m}}{(\bar{n}+1)^{n+m+1}}\frac{(R\bar{n}+1)^{m+1}}{(R\bar{n})^m} \\ &= \frac{(n+m)!}{n!m!}(1-R)^n\frac{\bar{n}^n(R\bar{n}+1)^{m+1}}{(\bar{n}+1)^{n+m+1}}. \end{aligned} \tag{C11}$$

This result is exact. If the numbers n, m are too large so that computation of the factorials is impractical, one can use an approximation based on the Stirling formula,

$$n! \approx \sqrt{2\pi n}\left(\frac{n}{e}\right)^n, \tag{C12}$$

to get (see Fig. 10)

$$\begin{aligned} p(n|m) &\approx \sqrt{\frac{n+m}{2\pi nm}}\left(\frac{n}{m}\right)^m\left(1+\frac{m}{n}\right)^{n+m} \\ &\quad\times(1-R)^n\frac{\bar{n}^n(R\bar{n}+1)^{m+1}}{(\bar{n}+1)^{n+m+1}}. \end{aligned} \tag{C13}$$

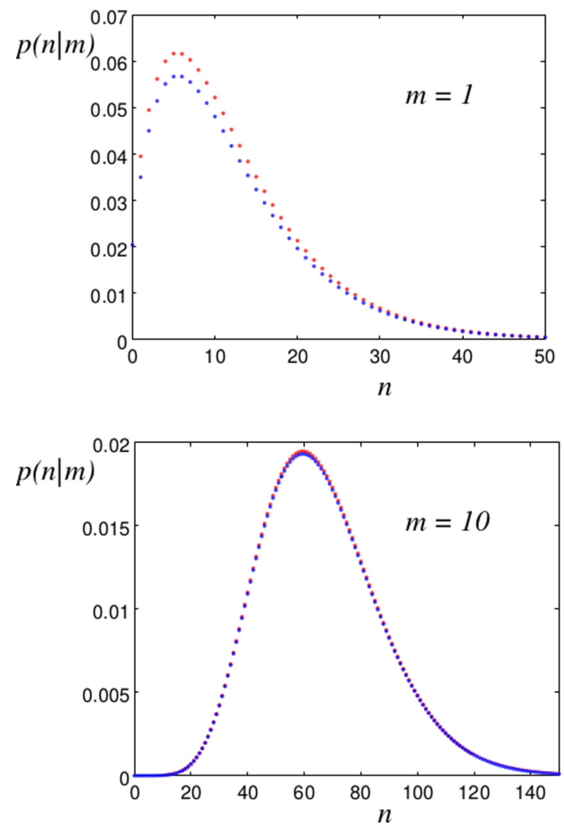

FIG. 10. Comparison of the exact conditional probability distribution $p(n|m)$ as in Eq. (C11) (blue) with the approximate formula of Eq. (C13) (red).

APPENDIX D: PHASE-PLANE DISTRIBUTION OF THE POSTMEASURED STATE FOLLOWING SMALL-FRACTION PHOTOCOUNT

The distribution of α, conditioned on the detection of quanta number m, is

$$P(\alpha|m) = \frac{p(m|\alpha)P(\alpha)}{p(m)}. \tag{D1}$$

The unmeasured (transmitted) field mode has the state (conditional on the detection of m)

$$\hat{\varrho}(n) = \frac{1}{\kappa^2}\int\int P\left(\frac{\alpha}{\kappa}|m\right)|\alpha\rangle\langle\alpha|d^2\alpha. \tag{D2}$$

In small-fraction photocount, the distribution of detected photons for a coherent state input $|\alpha\rangle$ yields a Poissonian statistics with the mean number of quanta $\lambda = (1-\kappa^2)|\alpha|^2$,

$$p(m|\alpha) = e^{-\lambda}\frac{\lambda^m}{m!}. \tag{D3}$$

In Eq. (D1), $p(m)$ is the quanta number distribution of a thermal state with mean quanta number $(1-\kappa^2)\bar{n}$, obtained according to Eq. (7).

APPENDIX E: WORK OPTIMIZATION FOR PHASE-SENSITIVE MEASUREMENT

Upon substituting $\xi = 2\beta^2$ and $\epsilon = 1-\kappa^2$, the work in Eq. (20) is optimized for

$$\xi = \frac{\sqrt{\bar{n}(1-\epsilon)}-1}{1+\frac{1}{\epsilon\bar{n}}} \tag{E1}$$

and

$$\epsilon = \frac{\sqrt{\bar{n}-\sqrt{\bar{n}}+1}-1}{\bar{n}}. \tag{E2}$$

Using these values, one gets the maximal extractable work in Eq. (21) as

$$W_{\max}/\hbar\omega \approx (\sqrt{\bar{n}-\sqrt{\bar{n}}+1}-1)^2\left(1-\frac{1}{\sqrt{\bar{n}}}\right). \tag{E3}$$

Let us optimize the extractable work in Eq. (90). Substituting $\xi = 2\beta^2$ and $\epsilon = 1-\kappa^2$, one can write Eq. (90) as

$$W/\hbar\omega = \frac{\bar{n}}{2\pi}\frac{1-\epsilon}{1+\frac{1}{\xi}+\frac{1}{\epsilon\bar{n}}} - \xi. \tag{E4}$$

Equating $\frac{\partial W}{\partial \xi} = 0$, we get a quadratic equation

$$\left(1+\frac{1}{\epsilon\bar{n}}\right)^2\xi^2 + 2\left(1+\frac{1}{\epsilon\bar{n}}\right)\xi + 1 - \bar{n}(1-\epsilon)/2\pi = 0, \tag{E5}$$

whose only positive root is given by

$$\xi = \frac{\sqrt{\bar{n}(1-\epsilon)/2\pi}-1}{1+\frac{1}{\epsilon\bar{n}}}. \tag{E6}$$

Substituting this in Eq. (E4), we get

$$W/\hbar\omega = \frac{\bar{n}\epsilon}{\bar{n}\epsilon+1}\left[\frac{\bar{n}}{2\pi}(1-\epsilon) - 2\sqrt{\frac{\bar{n}}{2\pi}(1-\epsilon)}+1\right]. \tag{E7}$$

For high transmittance BS using the approximation $\sqrt{1-\epsilon} \approx 1-\epsilon/2$, we get

$$W \approx \frac{\bar{n}\epsilon}{\bar{n}\epsilon+1}[(\sqrt{\bar{n}/2\pi}-\bar{n}/2\pi)y + (\sqrt{\bar{n}/2\pi}-1)^2]. \tag{E8}$$

Again equating $\frac{\partial W}{\partial \epsilon} = 0$, we get

$$\bar{n}\epsilon^2 + 2\epsilon - 1 + \sqrt{2\pi/\bar{n}} = 0. \tag{E9}$$

The above equation has only one positive root given by

$$\epsilon = \frac{\sqrt{\bar{n}-\sqrt{2\pi\bar{n}}+1}-1}{\bar{n}}. \tag{E10}$$

APPENDIX F: MUTUAL INFORMATION IN PHOTOCOUNT, HOMODYNE, AND SIGN WOF

Using Eqs. (43) and (44), we get

$$\mathcal{I} = -\sum_n p(n)S(p(m|n)) + S(p(m)). \tag{F1}$$

Here according to Bayes' theorem, the conditional probabilities follow:

$$p(m|n) = \frac{p(n|m)p(m)}{p(n)}. \tag{F2}$$

The Shannon entropy $S(p(i))$ associated with the probability distribution $p(i)$ is given as

$$S(p(i)) = -\sum_i p(i)\ln p(i). \tag{F3}$$

We have used Eq. (F1) for computing mutual information for the photocount WOF and sign measurement WOF. The sum is replaced by an integral where the continuum limit is applicable. We have considered natural logarithm instead of $\log_2$ in computing mutual information or entropy. However, as we are interested in calculating the erasing lower bound on the cost of the detector and feedforward cost, which are $k_BT_D\ln 2$ times the entropy and mutual information in bits (i.e., with $\log_2$), we compute I and I_D in natural logarithm units and multiply them by k_BT_D.

For calculating mutual information for the homodyne WOF, we have additionally considered properties of mutual information of two Gaussian distributions as detailed below. The mean mutual information generated in the detection process is given by Eqs. (38) and (39). Their explicit evaluation is effected by taking

$$P(x,p|\Delta n_x,\Delta n_p) \approx \frac{1}{2\pi\sigma_x^2}\exp\left[-\frac{(x-\bar{x}_{\Delta nx})^2+(p-\bar{p}_{\Delta np})^2}{2\sigma_x^2}\right], \tag{F4}$$

with

$$\bar{x}_{\Delta nx} = \frac{\Delta n_x}{\beta\sqrt{1-\kappa^2}\left[1+\frac{1}{\bar{n}(1-\kappa^2)}+\frac{1}{2\beta^2}\right]}, \tag{F5}$$

$$\bar{p}_{\Delta np} = \frac{\Delta n_p}{\beta\sqrt{1-\eta^2}\left[1+\frac{1}{\bar{n}(1-\kappa^2)}+\frac{1}{2\beta^2}\right]}, \tag{F6}$$

$$\sigma_x^2 = \frac{\bar{n}}{1+\frac{2\beta^2\bar{n}(1-\kappa^2)}{2\beta^2+\bar{n}(1-\kappa^2)}}. \tag{F7}$$

Equation (38) can be evaluated using the following property of a Gaussian distribution of variables X and Y in which the mutual information is given by

$$\langle I(X;Y)\rangle = -\frac{1}{2}\ln\left(1-\frac{\text{var}^2_{X,Y}}{\text{var}_X\,\text{var}_Y}\right). \tag{F8}$$

We find

$$\text{var}_{x,\Delta n_x} = \text{var}_{p,\Delta n_p} = \epsilon\sigma^2_{\Delta n} \tag{F9}$$

and

$$\text{var}_x = \text{var}_p = \bar{n}, \tag{F10}$$

$$\text{var}_{\Delta n_x} = \text{var}_{\Delta n_p} = \sigma^2_{\Delta n}, \tag{F11}$$

$$\sigma^2_{\Delta n} = \beta^2 + \bar{n}(1-\kappa^2)\left(\beta^2+\frac{1}{2}\right). \tag{F12}$$

For sign measurement WOF, $P(\Delta n_x,\Delta n_p|\alpha)$ in Eq. (65) can be approximated for large quanta number as [57]

$$P(\Delta n_x, \Delta n_p|\alpha) \approx \frac{1}{2\pi\left[\frac{(1-\kappa^2)|\alpha|^2}{2} + \beta^2\right]} \exp\left[-\frac{(\Delta n_x - \sqrt{2(1-\kappa^2)}\beta \,\mathrm{Re}\alpha)^2 + (\Delta n_p - \sqrt{2(1-\kappa^2)}\beta \,\mathrm{Im}\alpha)^2}{(1-\kappa^2)|\alpha|^2 + 2\beta^2}\right].$$

[1] F. Schwabl, *Statistical Mechanics* (Springer, Berlin, 2006).
[2] G. Kurizki and A. G. Kofman, *Thermodynamics and Control of Open Quantum Systems* (Cambridge University Press, Cambridge, UK, 2022).
[3] J. Gemmer, M. Michel, and G. Mahler, *Quantum Thermodynamics* (Springer-Verlag, Berlin, 2010).
[4] H. E. D. Scovil and E. O. Schulz-DuBois, Phys. Rev. Lett. **2**, 262 (1959).
[5] R. Kosloff and A. Levy, Annu. Rev. Phys. Chem. **65**, 365 (2014).
[6] R. Kosloff, Entropy **15**, 2100 (2013).
[7] D. Gelbwaser-Klimovsky, R. Alicki, and G. Kurizki, Phys. Rev. E **87**, 012140 (2013).
[8] D. Gelbwaser-Klimovsky, W. Niedenzu, and G. Kurizki, Adv. At. Mol. Opt. Phys. **64**, 329 (2015).
[9] T. Opatrný, S. Bräuer, A. G. Kofman, A. Misra, N. Meher, O. Firstenberg, E. Poem, and G. Kurizki, arXiv:2108.10157.
[10] M. O. Scully, M. S. Zubairy, G. S. Agarwal, and H. Walther, Science **299**, 862 (2003).
[11] R. Dillenschneider and E. Lutz, Europhys. Lett. **88**, 50003 (2009).
[12] C. Mukhopadhyay, A. Misra, S. Bhattacharya, and A. K. Pati, Phys. Rev. E **97**, 062116 (2018).
[13] S. De Liberato and M. Ueda, Phys. Rev. E **84**, 051122 (2011).
[14] X. L. Huang, T. Wang, and X. X. Yi, Phys. Rev. E **86**, 051105 (2012).
[15] O. Abah and E. Lutz, Europhys. Lett. **106**, 20001 (2014).
[16] H. Li, J. Zou, W.-L. Yu, B.-M. Xu, J.-G. Li, and B. Shao, Phys. Rev. E **89**, 052132 (2014).
[17] O. Abah, J. Roßnagel, G. Jacob, S. Deffner, F. Schmidt-Kaler, K. Singer, and E. Lutz, Phys. Rev. Lett. **109**, 203006 (2012).
[18] A. Ü. C. Hardal and Ö. E. Müstecaplıoğlu, Sci. Rep. **5**, 12953 (2015).
[19] C. B. Dag, W. Niedenzu, Ö. E. Müstecaplıoğlu, and G. Kurizki, Entropy **18**, 244 (2016).
[20] W. Niedenzu, D. Gelbwaser-Klimovsky, A. G. Kofman, and G. Kurizki, New J. Phys. **18**, 083012 (2016).
[21] D. Türkpençe and O. E. Müstecaplıoğlu, Phys. Rev. E **93**, 012145 (2016).
[22] S. Das, A. Misra, A. K. Pal, A. Sen(De), and U. Sen, Europhys. Lett. **125**, 20007 (2019).
[23] M. T. Naseem, A. Misra, and O. E. Müestecaplıoğlu, Quantum Sci. Technol. **5**, 035006 (2020).
[24] L. A. Correa, J. P. Palao, D. Alonso, and G. Adesso, Sci. Rep. **4**, 3949 (2014).
[25] W. Niedenzu, V. Mukherjee, A. Ghosh, A. G. Kofman, and G. Kurizki, Nat. Commun. **9**, 165 (2018).
[26] M. O. Scully, K. R. Chapin, K. E. Dorfman, M. B. Kim, and A. Svidzinsky, Proc. Natl. Acad. Sci. (USA) **108**, 15097 (2011).
[27] R. Uzdin, A. Levy, and R. Kosloff, Phys. Rev. X **5**, 031044 (2015).
[28] A. Ghosh, D. Gelbwaser-Klimovsky, W. Niedenzu, A. I. Lvovsky, I. Mazets, M. O. Scully, and G. Kurizki, Proc. Natl. Acad. Sci. (USA) **115**, 9941 (2018).
[29] K. Brandner, M. Bauer, and U. Seifert, Phys. Rev. Lett. **119**, 170602 (2017).
[30] W. Niedenzu and G. Kurizki, New J. Phys. **20**, 113038 (2018).
[31] A. Manatuly, W. Niedenzu, R. Román-Ancheyta, B. Çakmak, O. E. Müstecaplıoğlu, and G. Kurizki, Phys. Rev. E **99**, 042145 (2019).
[32] A. Ghosh, V. Mukherjee, W. Niedenzu, and G. Kurizki, Eur. Phys. J.: Spec. Top. **227**, 2043 (2019).
[33] J. Klatzow, J. N. Becker, P. M. Ledingham, C. Weinzetl, K. T. Kaczmarek, D. J. Saunders, J. Nunn, I. A. Walmsley, R. Uzdin, and E. Poem, Phys. Rev. Lett. **122**, 110601 (2019).
[34] J. Klaers, S. Faelt, A. Imamoglu, and E. Togan, Phys. Rev. X **7**, 031044 (2017).
[35] J. Roßnagel, O. Abah, F. Schmidt-Kaler, K. Singer, and E. Lutz, Phys. Rev. Lett. **112**, 030602 (2014).
[36] M. Esposito, R. Kawai, K. Lindenberg, and C. Van den Broeck, Phys. Rev. Lett. **105**, 150603 (2010).
[37] B. Gardas and S. Deffner, Phys. Rev. E **92**, 042126 (2015).
[38] A. Misra, U. Singh, M. N. Bera, and A. K. Rajagopal, Phys. Rev. E **92**, 042161 (2015).
[39] M. Campisi and R. Fazio, Nat. Commun. **7**, 11895 (2016).
[40] J. C. Maxwell, *Theory of Heat* (Longman, London, 1871).
[41] L. Szilard, Z. Phys. **53**, 840 (1929).
[42] R. Landauer, IBM J. Res. Dev. **5**, 183 (1961).
[43] C. H. Bennett, Int. J. Theor Phys. **21**, 905 (1982).
[44] J. M. R. Parrondo, J. M. Horowitz, and T. Sagawa, Nat. Phys. **11**, 131 (2015).
[45] M. D. Vidrighin, O. Dahlsten, M. Barbieri, M. S. Kim, V. Vedral, and I. A. Walmsley, Phys. Rev. Lett. **116**, 050401 (2016).
[46] T. Sagawa and M. Ueda, Phys. Rev. Lett. **100**, 080403 (2008).
[47] C. Elouard and A. N. Jordan, Phys. Rev. Lett. **120**, 260601 (2018).
[48] C. Elouard, D. Herrera-Martí, B. Huard, and A. Auffèves, Phys. Rev. Lett. **118**, 260603 (2017).
[49] A. E. Allahverdyan, R. Balian, and T. M. Nieuwenhuizen, Europhys. Lett. **67**, 565 (2004).
[50] W. Pusz and S. L. Woronowicz, Commun. Math. Phys. **58**, 273 (1978).
[51] D. Gelbwaser-Klimovsky, R. Alicki, and G. Kurizki, Europhys. Lett. **103**, 60005 (2013).
[52] R. Alicki, J. Phys. A **12**, L103 (1979).
[53] R. Uzdin and S. Rahav, Phys. Rev. X **8**, 021064 (2018).
[54] D. Gelbwaser-Klimovsky and G. Kurizki, Sci. Rep. **5**, 7809 (2015).
[55] D. Gelbwaser-Klimovsky and G. Kurizki, Phys. Rev. E **90**, 022102 (2014).

[56] A. Ghosh, C. L. Latune, L. Davidovich, and G. Kurizki, Proc. Natl. Acad. Sci. (USA) **114**, 12156 (2017).
[57] T. Opatrný, A. Misra, and G. Kurizki, Phys. Rev. Lett. **127**, 040602 (2021).
[58] H. Dong, A. Ghosh, M. B. Kim, S.-W. Li, A. A. Svidzinsky, Z. Zhang, G. Kurizki, and M. O. Scully, Eur. Phys. J.: Spec. Top. **230**, 867 (2021).
[59] Y. Guryanova, N. Friis, and M. Huber, Quantum **4**, 222 (2020).
[60] M. O. Scully and M. S. Zubairy, *Quantum Optics* (Cambridge University Press, Cambridge, UK, 1997).
[61] M. Nielsen and I. Chuang, *Quantum Computation and Quantum Information* (Cambridge University Press, Cambridge, UK, 2000).
[62] L. B. Kish and C. G. Granqvist, Europhys. Lett. **98**, 68001 (2012).
[63] R. H. Dicke, Phys. Rev. **93**, 99 (1954).
[64] R. H. Lehmberg, Phys. Rev. A **2**, 883 (1970).
[65] G. S. Agarwal, Quantum statistical theories of spontaneous emission and their relation to other approaches, in *Quantum Optics*, edited by G. Höhler (Springer, Berlin, 1974), pp. 1–128.
[66] A. V. Andreev, V. I. Emel'yanov, and Y. U. Il'inskii, *Cooperative Effects in Optics, Superradiance and Phase Transitions* (IOP, Bristol, 1993).
[67] I. E. Mazets and G. Kurizki, J. Phys. B **40**, F105 (2007).
[68] A. A. Svidzinsky, J.-T. Chang, and M. O. Scully, Phys. Rev. Lett. **100**, 160504 (2008).
[69] C. M. Natarajan, M. G. Tanner, and R. H. Hadfield, Supercond. Sci. Technol. **25**, 063001 (2012).
[70] M. A. Wolff, S. Vogel, L. Splitthoff, and C. Schuck, Sci. Rep. **10**, 17170 (2020).
[71] J. Yi, P. Talkner, and Y. W. Kim, Phys. Rev. E **96**, 022108 (2017).
[72] D. Gelbwaser-Klimovsky, N. Erez, R. Alicki, and G. Kurizki, Phys. Rev. A **88**, 022112 (2013).
[73] N. Erez, G. Gordon, M. Nest, and G. Kurizki, Nature **452**, 724 (2008).
[74] M. F. Anka, T. R. de Oliveira, and D. Jonathan, Phys. Rev. E **104**, 054128 (2021).
[75] G. Kurizki, M. Shapiro, and P. Brumer, Phys. Rev. B **39**, 3435 (1989).
[76] N. Bar-Gill, C. Gross, I. Mazets, M. Oberthaler, and G. Kurizki, Phys. Rev. Lett. **106**, 120404 (2011).
[77] C. Gross, H. Strobel, E. Nicklas, T. Zibold, N. Bar-Gill, G. Kurizki, and M. K. Oberthaler, Nature **480**, 219 (2011).
[78] G. Kurizki and M. Shapiro, J. Opt. Soc. Am. B **8**, 355 (1991).
[79] *Phononic Crystals: Fundamentals and Applications*, 1st ed., edited by A. Khelif and A. Adibi (Springer, Berlin, 2015).
[80] *Acoustic Metamaterials and Phononic Crystals*, 2013th ed., edited by P. A. Deymier (Springer, Berlin, 2013).
[81] M. S. Kushwaha, P. Halevi, L. Dobrzynski, and B. Djafari-Rouhani, Phys. Rev. Lett. **71**, 2022 (1993).
[82] A. Khelif, B. Djafari-Rouhani, J. O. Vasseur, and P. A. Deymier, Phys. Rev. B **68**, 024302 (2003).
[83] T. Elnady, A. Elsabbagh, W. Akl, O. Mohamady, V. M. Garcia-Chocano, D. Torrent, F. Cervera, and J. Sánchez-Dehesa, Appl. Phys. Lett. **94**, 134104 (2009).